Transaction A: Civil Engineering
Vol. 16, No. 6, pp. 443–456

SCIENTIA
IRANICA

Passive Devices for Wave Induced Vibration Control in Offshore Steel Jacket Platforms

A.A. Golafshani[1,*] **and A. Gholizad**[2]

Abstract. *Performances of tuned mass dampers and friction dampers to mitigate the wave induced vibrations in jacket type offshore platforms have been compared in this study. Due to the random nature of ocean waves, a full stochastic analysis method has been used to evaluate the response of the structures equipped with these devices. A stochastic linearization technique has been used to take the nonlinear behavior of friction dampers into account. The developed mathematical formulation has been applied to evaluate the response of realistic models, and to find out the optimal values for the adjustable parameters of friction dampers. The results have been verified in comparison with time domain nonlinear analyses results. Also, a computer utility has been provided in FORTRAN to perform the spectral fatigue analysis of platforms and together with a Genetic Algorithm utility, it has been used to find out the optimal parameters of a tuned mass damper to dissipate the wave induced vibrations of the platforms. Although the efficiency of both dissipative systems increases for more flexible platforms due to the dominancy of the dynamic response, the functionality of TMD devices is more dependent on the dynamic characteristics of the platform; friction dampers seem to be more efficient for fixed steel jacket platforms.*

Keywords: *Steel jacket platforms; Power spectral analysis; Friction damper; Stochastic linearization; Tuned mass damper; Genetic algorithm.*

INTRODUCTION

Novel types of vibration control mechanisms have been widely studied and some have been implemented to improve the dynamic behavior of structures. However, comprehensive review of these studies, reported by Spencer and Nagarajaiah [1], shows that most of this research has focused on the protection of tall buildings and long span bridges against seismic or wind excitations. Only a small part of this research is related to fixed offshore platforms.

The first group of studies on this topic was published by Abdel-Rohman [2], who investigated the efficiency of some active and passive control mechanisms to moderate the dynamic response of a steel jacket platform due to wave-induced forces. Terro et al. [3] employed an active tuned mass damper with velocity feedback to minimize deck displacements in a sample steel jacket platform. Suhardjo and Kareem [4] tried some active control mechanisms, such as active tendons. Subsequently, Li et al. [5] made some improvements in their methodology. Zribi et al. [6] used the Lyapanov theory and a state feedback robust control to design an active tuned mass damper. Hui Ma et al. [7] considered the AMD mechanism and designed a control law with a feedforward and feedback optimal control algorithm to reduce the displacement and velocity responses of jacket type offshore platforms.

Fatigue damage is the most important criteria for joint design in offshore platforms located in areas with relatively high ratios of operational sea-states to maximum design environmental events. Therefore, utilizing control mechanisms with the aim of increasing fatigue life may be more preferable to mere deck displacement and acceleration control. Moreover, considering the excessive cost of underwater fabrication and welding, using a control mechanism to improve the fatigue life of existing offshore platforms, which are overloaded with extra piping and equipment, would be an attractive idea.

Since the control mechanism used for fatigue damage mitigation will interact with the main structure

1. *Department of Civil Engineering, Sharif University of Technology, P.O. Box 11155-9313, Tehran, Iran.*
2. *Department of Civil Engineering, University of Mohaghegh Ardebili, Ardebil, P.O. Box 56199-11367, Iran.*
*. *Corresponding author. E-mail: golafshani@sharif.edu*

Received 17 November 2008; accepted 24 August 2009

during a considerable part of the platform life span, implementation of an active control technique with a permanent power source would not be practical in such cases; utilizing some kind of passive or semi-active control mechanisms that can be installed on existing platforms is often preferable.

Moreover, considering the excessive cost of underwater fabrication and welding, which obstructs practical techniques for the rehabilitation of offshore platforms, the use of passive control mechanisms would be an attractive idea to improve the dynamic behavior of existing offshore platforms.

In a passive control approach, Hsien Hua Lee [8] utilized viscoelastic dampers as bracings to improve the dynamic performance of an offshore platform, and Patil and Jangid [9] compared the efficiency of viscoelastic, viscous and friction dampers as energy dissipating devices to moderate the dynamic response of steel jacket platforms. They have considered an additional stiffness and damping due to the utilization of viscoelastic and viscous dampers, but the system of inclusion of the nonlinear behavior of friction dampers in spectral analyses has not been clarified in their published article.

A TMD was ordered in 2005 to be designed for the seismic rehabilitation of the Sakhalin-I drilling platform and it is the only reported offshore application of TMD devices.

Power spectral analysis is one of the most conventional methods for the analysis of offshore structures under random wave excitation. It yields more realistic and reliable results, especially for long-term fatigue analysis and is therefore recommended in most offshore engineering standards. The linear time invariant response of the structure and zero mean stationary Gaussian random excitation are principal assumptions in this approach; hence, the practice of this method for nonlinear structures needs proper approximating techniques, such as the Fokker-Plank method and stochastic linearization [10]. The theoretical basis for the last one was firstly introduced by Booton, Kazakov [10] and Caughey [11] in the 1950s and has found extensive applications in the stochastic analysis of nonlinear dynamic systems. An extensive review of the studies on this topic [12] and an introduction to some of its practical applications have been reported by Socha [13]. The stochastic linearization technique exercised in this study relies on the minimization of the mean square error which was first introduced by Atalik and Utku [14].

SCOPE OF THE CURRENT STUDY

The objective of this paper is to evaluate the performance of fixed offshore platforms, utilized with some passive devices and excited by random wave induced forces. Full stochastic spectral analysis has been used for this purpose and a stochastic linearization method has been employed to take the nonlinear behavior of friction dampers into consideration. Time domain nonlinear analyses have been performed, as well, to verify the results of this approximate method. An artificial record of sea wave time history has been generated in accordance with the considered PSD function, and the structural model has been analyzed under resultant lateral loading using Open-Sees software, which facilitates the modeling of nonlinear and hysteretic element behavior.

TMD efficiency for the dissipation of wave induced vibrations has been examined using a simplified lumped mass model of platforms. Also, a computer utility has been provided in FORTRAN to perform a more precise power spectral fatigue analysis of platforms and has been used together with a genetic algorithm utility to find out the optimal parameters of tuned mass dampers. Topside displacement has been considered as an objective function for this minimization problem and TMD tuning and damping ratios are the adjustable parameters of this device, which have been considered as optimization parameters. Explicit inclusion of the dynamic characteristics of TMD necessitates the consideration of non-classical damping in the structural analysis. The prepared program has been validated in comparison with existing reliable software.

This study has been done with the aim of appreciation passive vibration control devices to mitigate the accumulative fatigue damage in steel jacket type platforms.

FRICTION DAMPERS

Friction dampers are passive control devices with an effective performance in energy dissipation including relatively low cost and ease of installation. The displacement-dependency of the energy dissipation rate in friction dampers is a major difference between these and other types of damping device. Their resultant damping force is independent of the velocity response of the structure and the frequency content of excitations and this makes them suitable for low frequency excitations, such as sea wave loading. Highly nonlinear and force limited action is the dominant characteristic of these devices. Diversiform friction dampers with various configurations have been invented and utilized for vibration control applications with a few practical applications against seismic excitations.

A novel friction damper device, which can be easily installed on existing structures, has been innovated by Mualla and Belev [15]. They have presented an analytical description of its behavior that follows an idealized hysteretic loop as shown in Figure 1.

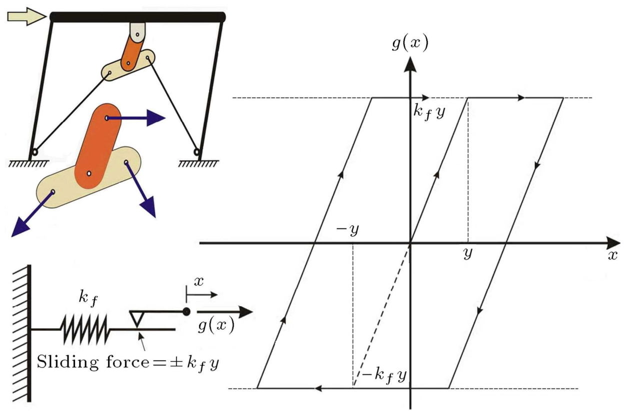

Figure 1. Configuration of friction damper innovated by Mualla and Belev [15].

Hysteretic Devices Under Random Excitations

The governing equations of motion for the structure utilized with friction dampers can be derived from the schematic diagram as shown in Figure 2, and can be written as Equation 1 in which $[M]$, $[C]$ and $[K]$ are the mass, damping and stiffness matrices of the primary structure, respectively:

$$[M]\{\ddot{x}\} + [C]\{\dot{x}\} + [K]\{x\} + \{g\} = \{f\}, \tag{1}$$

$$[C] = \frac{2\xi_i}{\omega_i}[K], \qquad i = 1, \cdots, n, \tag{2}$$

$$\{x\} = \{x_n(t), x_{n-1}(t), \cdots, x_1(t)\}^T, \tag{3}$$

$$\{g\} = \{g_n(t), g_{n-1}(t), \cdots, g_1(t)\}^T,$$

$$\{f\} = \{f_n(t), f_{n-1}(t), \cdots, f_1(t)\}^T. \tag{4}$$

where ξ_i and ω_i are the damping ratio and the natural frequency of the ith vibration mode; $g_n(t)$, is the hysteretic restoring force resulted from the nth friction damper as shown in Figure 2; and $f_n(t)$ is the random environmental excitation on the nth degree of freedom.

One needs to introduce some additional appropriate variables $\{z\}$ as shown in Figure 2 to express the restoring forces, $g_n(t)$, as an explicit and non-hysteretic function of the new set of variables:

$$g_n(t) = k_{fn}[z_n(t) - x_{n-1}(t)]. \tag{5}$$

The sliding phase in the friction damper deformation begins when $z_n(t) - x_{n-1}(t)$ reaches $\pm y_n$ and, at this stage $\dot{z}_n(t) - \dot{x}_{n-1}(t)$ changes to zero from its value of $\dot{x}_n(t) - \dot{x}_{n-1}(t)$ in the sticking phase. The sliding phase terminates when $\dot{x}_n(t) - \dot{x}_{n-1}(t)$ reverses its sign and the value of the restoring force moves back from $\pm\, k_{fn}y_n$ toward zero.

A classical way for an approximate solution of the vibration in a randomly excited nonlinear system is the method of stochastic linearization, in which the nonlinear equation of motion is replaced by an equivalent linear one. The differences between the nonlinear equations and their linear equivalents are zero mean stochastic processes, which have been considered as error functions. The variances of these error functions should be minimized in the linearization technique that has been used in this article. The following linear forms

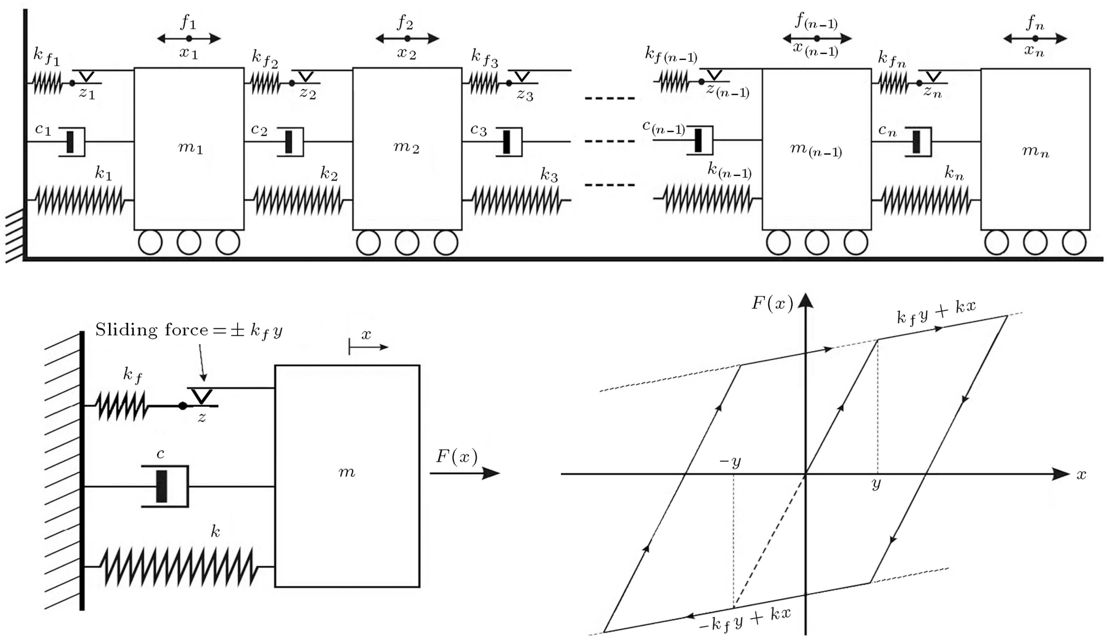

Figure 2. Force-deformation diagram for friction damper after Mualla and Belev [15].

have been introduced in this problem:

$$\begin{aligned}\dot{z}_n(t)-\dot{x}_{n-1}(t)&=a_n(z_n(t)-x_{n-1}(t))\\&\quad+b_n(\dot{x}_n(t)-\dot{x}_{n-1}(t))\\&\quad+c_n(x_n(t)-x_{n-1}(t))+d_n,\end{aligned}\tag{6}$$

$$\begin{aligned}g_n(t)&=k_{fn}(z_n(t)-x_{n-1}(t))\\&=p_n(z_n(t)-x_{n-1}(t))\\&\quad+q_n(\dot{x}_n(t)-\dot{x}_{n-1}(t))\\&\quad+r_n(x_n(t)-x_{n-1}(t))+s_n.\end{aligned}\tag{7}$$

With the assumption of $\{x(t)\}$ and $\{z(t)\}$ as jointly zero mean Gaussian processes, applying the linearization technique [14] will result in:

$$\begin{aligned}a_n&=E\left[\frac{\partial(\dot{z}_n(t)-\dot{x}_{n-1}(t))}{\partial(z_n(t)-x_{n-1}(t))}\right]\\&=-2\int_0^\infty \upsilon p_{\dot{x}_n(t)-\dot{x}_{n-1}(t),z_n(t)-x_{n-1}(t)}(\upsilon,y_n)d\upsilon,\end{aligned}\tag{8}$$

$$\begin{aligned}b_n&=E\left[\frac{\partial(\dot{z}_n(t)-\dot{x}_{n-1}(t))}{\partial(\dot{x}_n(t)-\dot{x}_{n-1}(t))}\right]\\&=1-2\int_{y_n}^\infty\int_0^\infty p_{\dot{x}_n(t)-\dot{x}_{n-1}(t),z_n(t)-x_{n-1}(t)}(\upsilon,\eta)d\upsilon d\eta,\end{aligned}\tag{9}$$

$$c_n=E\left[\frac{\partial(\dot{z}_n(t)-\dot{x}_{n-1}(t))}{\partial(x_n(t)-x_{n-1}(t))}\right]=0,\tag{10}$$

$$d_n=E(\dot{z}_n(t)-\dot{x}_{n-1}(t))=0.\tag{11}$$

Using a jointly Gaussian probability density function for $p_{\dot{x}_n(t)-\dot{x}_{n-1}(t),z_n(t)-x_{n-1}(t)}$ gives the following expressions for the coefficients of the aforementioned linearized equations:

$$a_n=-2\frac{\sigma_{\dot{x}_n-\dot{x}_{n-1}}}{\sigma_{z_n-x_{n-1}}}\hat{a}_n,\tag{12}$$

$$\begin{aligned}\hat{a}_n&=\frac{Y_n\rho_{\dot{x}_n(t)-\dot{x}_{n-1}(t),z_n(t)-x_{n-1}(t)}}{\sqrt{2\pi}}\exp\left(\frac{-Y_n^2}{2}\right)\\&\quad\times\Phi\left(\frac{Y_n\rho_{\dot{x}_n(t)-\dot{x}_{n-1}(t),z_n(t)-x_{n-1}(t)}}{R_n}\right)\\&\quad+\frac{R_n}{2\pi}\exp\left(\frac{-Y_n^2}{2R_n^2}\right),\end{aligned}\tag{13}$$

$$\begin{aligned}Y_n&=\frac{y_n}{\sigma_{z_n-x_{n-1}}},\\R_n&=\sqrt{1-\rho^2_{\dot{x}_n(t)-\dot{x}_{n-1}(t),z_n(t)-x_{n-1}(t)}},\\b_n&=1-2\int_{y_n/\sigma_{z_n-x_{n-1}}}^\infty\frac{e^{-r^2/2}}{\sqrt{2\pi}}\Lambda dr,\\\Lambda&=\Phi\left(\frac{r\rho_{\dot{x}_n(t)-\dot{x}_{n-1}(t),z_n(t)-x_{n-1}(t)}}{\sqrt{1-\rho^2_{\dot{x}_n(t)-\dot{x}_{n-1}(t),z_n(t)-x_{n-1}(t)}}}\right).\end{aligned}\tag{14}$$

Doing the same for p_n, q_n, r_n and s_n leads to:

$$p_n=k_{fn}b_n,\tag{15}$$

$$q_n=-2k_{fn}\frac{\sigma_{z_n-x_{n-1}}}{\sigma_{\dot{x}_n-\dot{x}_{n-1}}}\hat{q}_n,\tag{16}$$

$$\hat{q}_n=\frac{-Y_n}{\sqrt{2\pi}}\Phi\left(\frac{-Y_n}{R_n}\right)+\frac{R_n}{2\pi}\exp\left(\frac{-Y_n^2}{2R_n^2}\right),\tag{17}$$

$$r_n=0,\tag{18}$$

$$s_n=0.\tag{19}$$

Since only the steady state response is of interest to us and in order to escape from time domain methods, one can use a state-space representation of this system, as given by:

$$\dot{Y}+AY=Q.\tag{20}$$

The state vector, Y, and state matrix, A, may be described by:

$$Y=\begin{Bmatrix}z_n-x_{n-1}\\\vdots\\z_2-x_1\\z_1\\x_n-x_{n-1}\\\vdots\\x_2-x_1\\x_1\\\dot{x}_n-\dot{x}_{n-1}\\\vdots\\\dot{x}_2-\dot{x}_1\\\dot{x}_1\end{Bmatrix},$$

$$Q=\begin{Bmatrix}\{0\}\\\{0\}\\[M]^{-1}_{n\times n}\{f\}_{n\times 1}\end{Bmatrix},$$

$$A=\begin{bmatrix} -[a]_{n\times n} & [0]_{n\times n} & -[b]_{n\times n} \\ [0]_{n\times n} & [0]_{n\times n} & -[I]_{n\times n} \\ [M]^{-1}_{n\times n}[p]_{n\times n} & [M]^{-1}_{n\times n}[K]_{n\times n} & [M]^{-1}([C]_{n\times n}+[q]_{n\times n}) \end{bmatrix}. \tag{21}$$

Since the wave excitations and the resultant responses of offshore structures can be modeled by zero mean Gaussian processes, the second moment autocorrelation and covariance functions give a complete description of such stochastic processes. Therefore, these parameters are required to be found for the response of the structure.

Right Multiplying the state space equation of motion by Y^T and adding the resultant equation with its own transpose leads to a new equation. Taking the expected value of both sides of this equation gives the state space covariance equation:

$$\frac{d}{dt}E(YY^T)+AE(YY^T)+E(YY^T)A^T = E(QY^T)+E(YQ^T). \tag{22}$$

The first term of this equation refers to the non-stationary part of the response, which can be neglected, considering the stationary part of the response only. Trying to simplify this equation, one can substitute the right hand side of Equation 22:

$$E[Q(t)Y^T(t)]=E[Q(t)Y^T(0)]+\int_0^t E[Q(t)Q^T(\tau)]d\tau - A\int_0^t E[Q(t)Y^T(\tau)]d\tau. \tag{23}$$

Since the response at each time is not affected by excitations which will occur at the coming times, then $Y(0)$ is independent of $Q(t)$ and the first and last terms of the aforementioned equation can be eliminated as follows:

$$E[Q(t)Y^T(t)] = \int_t^0 E[Q(t)Q^T(t-s)]ds = \int_0^t R_{QQ}(s)ds, \tag{24}$$

where $R_{QQ}(s)$ is the autocorrelation function of the excitation with a power spectral density function of $S_{QQ}(\omega)$:

$$R_{QQ}(s)=\int_{-\infty}^{+\infty} S_{QQ}(\omega)e^{i\omega s}d\omega. \tag{25}$$

The same result can be derived similarly for $E[Y(t)Q^T(t)]$ and Equation 26 can be rewritten as:

$$AE(YY^T)+E(YY^T)A^T = 2\int_0^{+\infty}\int_{-\infty}^{+\infty} S_{QQ}(\omega)e^{i\omega s}d\omega ds. \tag{26}$$

$E(YY^T)$ is a symmetric matrix which contains all variances and the covariance of state variables. If friction dampers are utilized in n_f stories, $N=2\times n+n_f$ state variables will be required to formulate the problem associated with the stochastic vibration of such a system. The above presented equation is symmetric on both sides, so a set of $N(N+1)/2$ simultaneous nonlinear scalar algebraic equations are available that are coupled with $3\times n_f$ nonlinear equations consequent on Equations 11, 13 and 15.

n equations, corresponding to components (n_f+i, n_f+n+i), $i=1,\cdots,n$ of Equation 26, lead to $E((x_i-x_{i-1})(\dot{x}_i-\dot{x}_{i-1}))=0$, $i=1,\cdots,n$ which is evident for any stationary process as (x_i-x_{i-1}). Also, components (i,i) $i=1,\cdots,n_f$ yield:

$$a_iE((z_i-z_{i-1})^2)+b_iE((z_i-z_{i-1})(\dot{x}_i-\dot{x}_{i-1}))=0, \quad i=1,\cdots,n. \tag{27}$$

Substitution of these equations with Equation 12 results in:

$$2\hat{a}_i-b_i\rho_{z_i-z_{i-1},\dot{x}_i-\dot{x}_{i-1}}=0, \qquad i=1,\cdots,n. \tag{28}$$

This equation may be solved together with Equations 13 and 14 to give $\rho_{z_n-z_{n-1},\dot{x}_n-\dot{x}_{n-1}}$, $\hat{a}_n$, b_n and $\hat{q}_n$ as functions of $y_n/\sigma_{z_n-x_{n-1}}$ which have been shown in Figure 3.

These simplifications facilitate the solution of the main problem for every $y_n/\sigma_{z_n-x_{n-1}}$. Although this set of scalar equations can be solved with numerical methods, its complexity quickly diminishes when the friction devices are to be installed at a few stories.

WAVE FORCES MODELING AND TIME DOMAIN ANALYSES

Knowing the water particle velocity and acceleration in the vector notation, the wave induced forces on a cylindrical member can be calculated by the Morrison equation. The linearized form of the Morrison equation is [16]:

$$p(t)=\rho C_m V\dot{U}_n(t)+\frac{1}{2}\rho C_d A\sigma_u\sqrt{\frac{8}{\pi}}U_n(t), \tag{29}$$

where $p(t)$ is wave force per unit length of the member; C_d and C_m are drag and inertia coefficients,

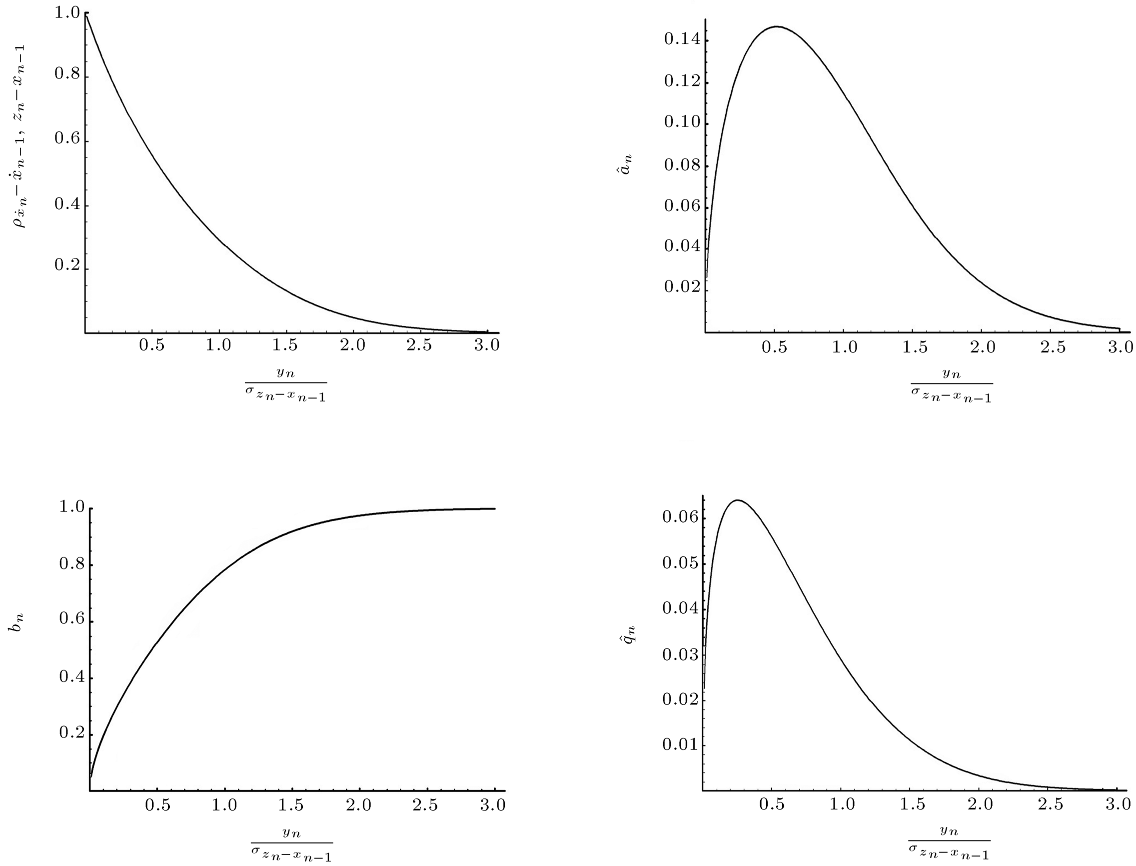

Figure 3. $\rho_{z_n - z_{n-1}, \dot{x}_n, \dot{x}_{n-1}}$, $\hat{a}$, b_n and $\hat{q}$ as functions of $y_n/\sigma_{z_n - x_{n-1}}$.

respectively; V and A are the displaced volume of the cylinder and the projected area normal to the member axis, both per unit length of the member; ρ is sea water density; $U_n(t)$ refers to the velocity of the fluid normal to the structural member which can be derived according to relevant wave theories; and σ_u is the standard deviation of the velocity.

$H_{f\zeta}(\omega)$ is defined as the transfer function from wave height to the resultant force on the unit length of a cylindrical member. Considering wave height as a zero mean stationary random process with power spectral density function $S_\zeta(\omega)$, the PSD function of the hot spot stress, $S_f(\omega)$, can be obtained as:

$$S_f(\omega) = |H_{f\zeta}(\omega)|^2 \, S_\zeta(\omega). \tag{30}$$

The most popular wave spectrum that is especially suited for open sea areas is well known as the Pierson-Moskowitz wave spectrum [16] and is used in this study as:

$$S_\zeta(\omega) = \frac{124.37 H_s^2}{T_z^4} \omega^{-5} \exp\left(\frac{-497.5}{T_z^4} \omega^{-4} \right), \tag{31}$$

in which H_s is significant wave height and T_z is the wave zero up crossing period. To validate the results of the stochastic linearization method, time domain nonlinear analyses have been performed using artificially generated sea waves recorded in accordance with the considered PSD function. The following equation is the basis for generation of the so-called artificial random record [17].

$$\eta(x,t) = \sum_{n=1}^{N} \sqrt{4 S_{\eta\eta}(\omega_n) \Delta\omega} \cos(k_n x - \omega_n t + \theta_n). \tag{32}$$

θ_n is the random phase angle from the interval between 0 and 2π. An original PSD function, artificially generated record and regenerated PSD function are shown in Figure 4.

The nonlinear behavior of a friction damper has been modeled in OpenSees software. Analysis results under cyclic loading have been compared with the results reported by Mualla et al. [15] to validate the OpenSees model. The results which are available from Figure 5, denote an acceptable conformity.

NUMERICAL RESULTS

In the current study, the usage of friction devices has been examined to moderate the dynamic response of

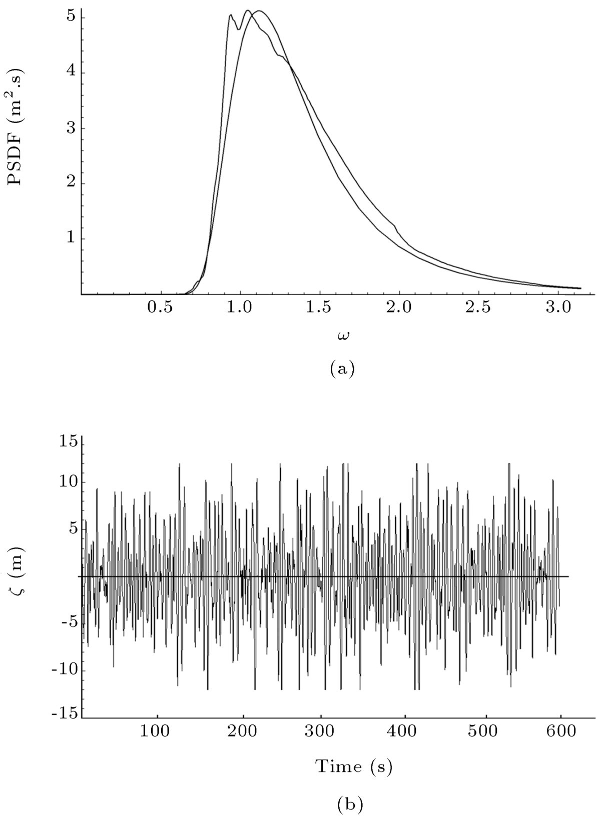

Figure 4. a) Original and regenerated PSDF b) Artificially generated wave record.

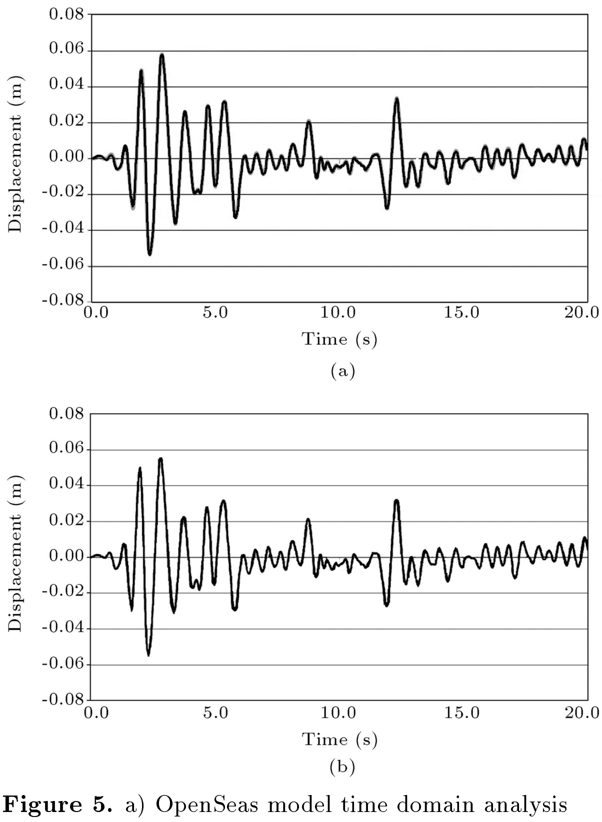

Figure 5. a) OpenSeas model time domain analysis result; b) Analysis result after Mualla and Belev [15].

three realistic jacket type platforms shown in Figure 6. The first one is the North Rankin "B" platform, which has been designed to be located at a 125 meter depth of water in Western Australia. The second one is the 95 meter high "Foroozan" six leg platform, which has been located in the Persian Gulf. The ponderous topsides of these two platforms have been installed with a float-over technique, which requires the omission of bracings at sea water level in one direction. This causes relatively high flexibility for the upper elevation of the platform in that direction. Therefore, the auxiliary friction device has been utilized in this position for these two platforms. The last one is a four leg, K braced jacket type platform at a water depth of 68 meters whose structural characteristics have been taken from Dalane [18]. All existing K braces have been utilized with friction dampers to evaluate their efficiency on this platform.

The structural model of the platforms has been simplified as a multi-degree of freedom system. An adequate number of modes have been considered such that a satisfactory value of the accumulative mass participation factor of the main structures vibrations is included. The lumped mass values and structural stiffness, as shown in Table 1, have been determined in a manner to provide the same natural period and kinetic energy for each intended mode of vibration.

The numerical solution of nonlinear equations corresponding to these systems and consequent on

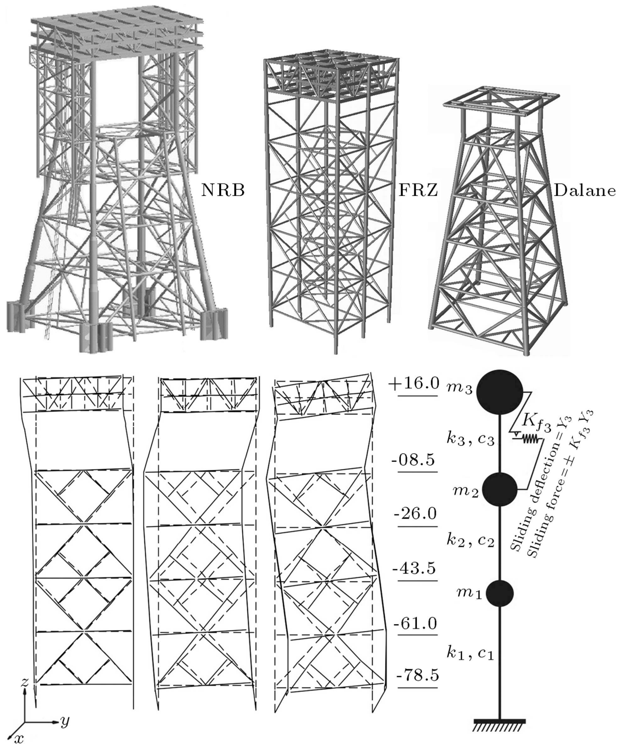

Figure 6. Sample steel jacket platforms, dynamic mode shapes and simplified MDF system.

Table 1. Sample platforms dynamic characteristics.

	Platforms		
	NRB	**FRZ**	**Dalane**
Period (Sec.)	4.8	2.7	1.5
$\boldsymbol{K_1}$ **(MN/m)**	400	335	58
$\boldsymbol{K_2}$ **(MN/m)**	430	365	50
$\boldsymbol{K_3}$ **(MN/m)**	39	32	53
$\boldsymbol{m_1}$ **(Ton)**	9000	1450	1000
$\boldsymbol{m_2}$ **(Ton)**	11000	2050	1200
$\boldsymbol{m_3}$ **(Ton)**	31000	6100	3100

Equation 26 results in six sets of solution. Only one of these solutions leads to real and positive values for probabilistic variables of this problem according to all values of $y_3/\sigma_{z_3-x_2}$. The results related to this solution are shown in Figure 7, which shows the variance of FRZ topside displacement according to different values for the adjustable parameters of the hysteretic device; also the variance of topside velocity changes in a similar manner. The variance of topside displacement is an important value, especially in the power spectral analysis of offshore platforms, because of its direct correlation with accumulative fatigue damage.

The concavity of these surfaces implies optimal values for adjustable parameters of the friction damper. These optimal values are clear in the following diagrams and are definitely dependent on the dynamic characteristics of the primary structure and also on the intensity of environmental excitations. An optimal value of $Y_3 = 0.85 \times \sigma_{Z_3-X_2}$ for the sliding initiation deflection of the auxiliary system is inferred in Figure 8 for FRZ and the optimal value of $Y_3 = 0.9 \times \sigma_{Z_3-X_2}$

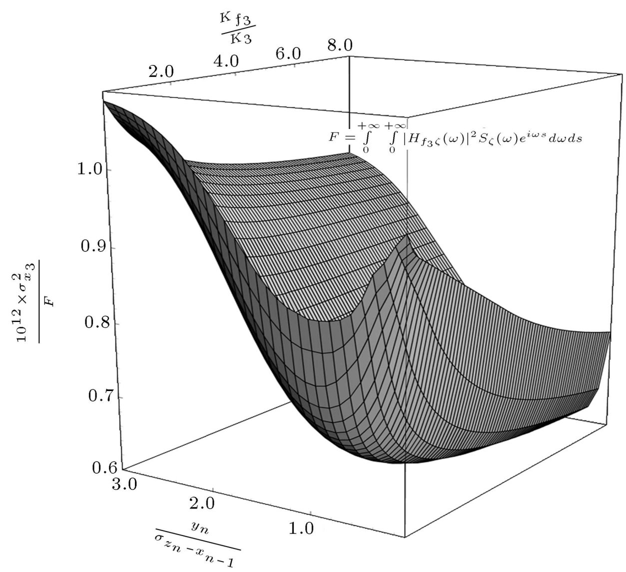

Figure 7. Topside displacement variance for different regulations of friction damper.

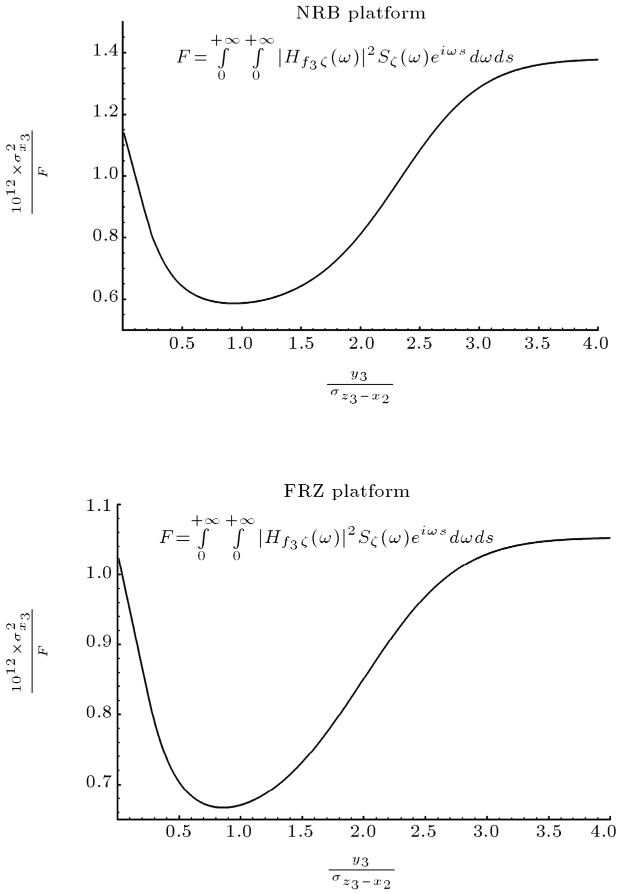

Figure 8. Topside displacement variance for different tuning of friction damper.

for NBR. The same optimal values are resulted for the response velocity control according to Figure 9. Since $\sigma_{Z_3-X_2}$ is dependent on the intensity of excitations, this optimal value for Y_3 will increase for more intense sea states. The allocation of higher values for the sliding deflection of the friction damper leads to more exertion of auxiliary bracings. It can be understood from Figure 10 that they will act as ordinary bracings for $Y_3 > 3.0 \times \sigma_{Z_3-X_2}$. Also, the optimum stiffness of the auxiliary system in its sticking phase may be drawn from Figure 11, as $K_{f3} = 3.85 \times K_3$ for FRZ and $K_{f3} = 4.2 \times K_3$ for NRB. The efficiency of the hysteretic system is more sensitive to the tuning of the sliding initiation deflection rather than to the bracing stiffness, and deviation from its optimal value may lead to the ineffectiveness of the friction damper.

The utilization of an optimally tuned friction damper on FRZ and NRB platforms resulted in a 36% and 48% reduction in the variance of the topside displacement, respectively, also a 40% reduction in the variance of its velocity. This represents the effectiveness of this device to moderate the dynamic response of offshore platforms subject to wave induced excitations. The utilization of auxiliary devices on the third platform does not exhibit a remarkable performance

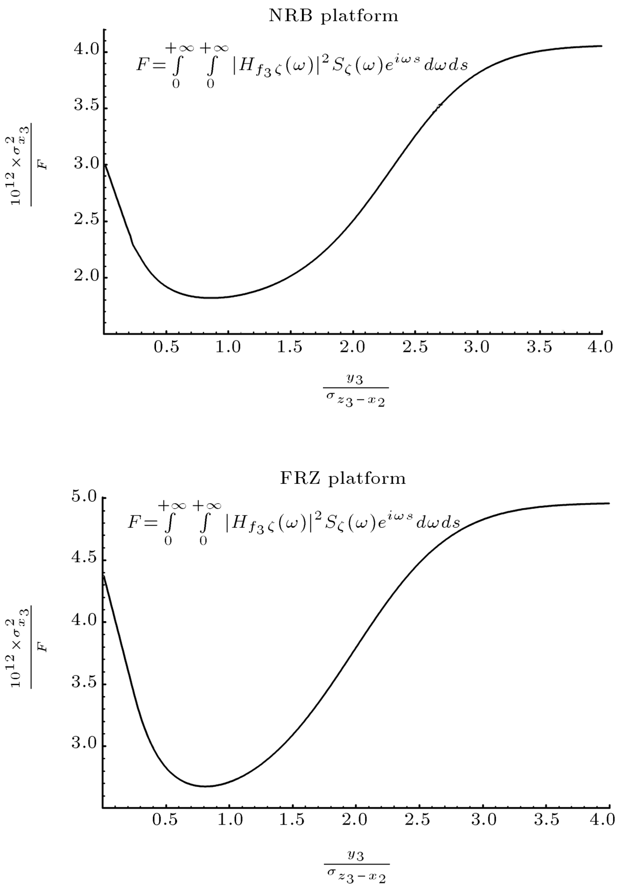

Figure 9. Topside velocity variance for different tuning of friction damper.

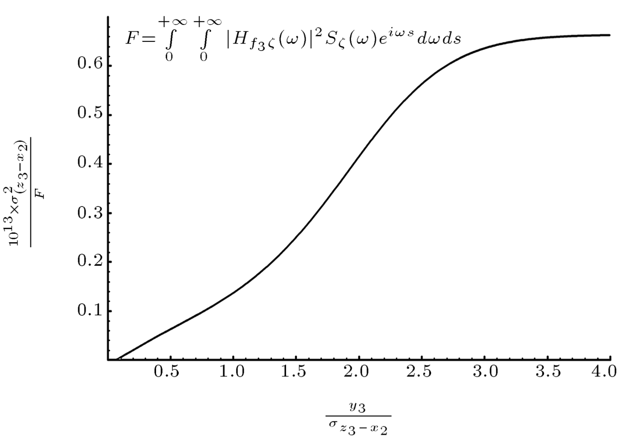

Figure 10. Auxiliary bracing deflection variance for different tuning of the friction damper.

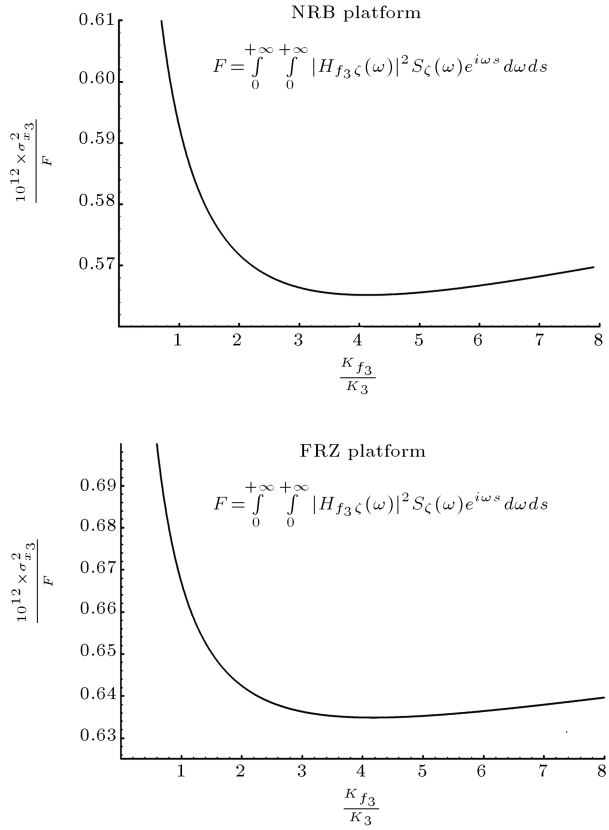

Figure 11. Topside displacement variance for different stiffness in sticking phase.

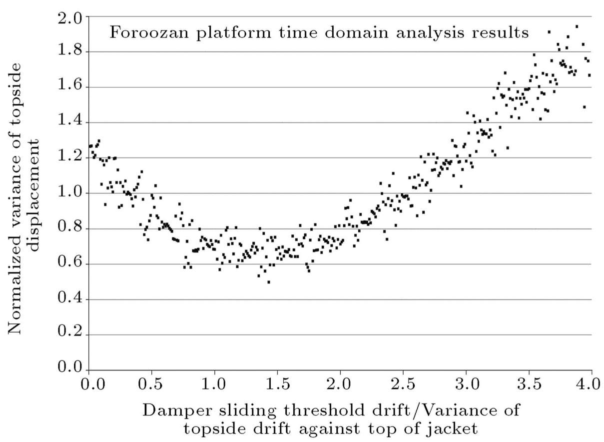

Figure 12. Time domain analysis result for the platform utilized with friction damper

for vibration control and only a 16% reduction in the topside displacement variance has been resulted in the best regulation of the friction devices. It is mostly due to the rigidity of this platform and its quasi-static response.

Sample platform models have also been analyzed in the time domain considering different adjustments for friction dampers. Comparative results, which have been summarized for the Foroozan platform in Figure 12, comply with the results in Figure 8.

TMD Equipped Platform Under Wave Excitations

TMDs are simple passive control devices which have been installed on a large number of civil structures some of which have been listed by Holmes [19]. TMDs have been found to be reliable and effective in reducing the vibration response of excited structures. They exude a good performance to control a single mode of structural vibration that can be demonstrated with a single degree of freedom system. Therefore, the derivation of closed form expressions for optimum tuning and damping ratios that are available in literature, has been based on the equation of motion of an SDOF system equipped with a TMD as shown in Figure 13.

$$\begin{bmatrix} 1+\mu & \mu \\ \mu & \mu \end{bmatrix} \begin{Bmatrix} \ddot{x} \\ \ddot{y} \end{Bmatrix} + \begin{bmatrix} 2\xi_x\omega_x & 0 \\ 0 & 2\xi_y\omega_y \end{bmatrix} \begin{Bmatrix} \dot{x} \\ \dot{y} \end{Bmatrix} + \begin{bmatrix} 2\xi_x\omega_x & 0 \\ 0 & 2\xi_y\omega_y \end{bmatrix} \begin{Bmatrix} x \\ y \end{Bmatrix} = \begin{Bmatrix} f_x/m_x \\ 0 \end{Bmatrix}, \tag{33}$$

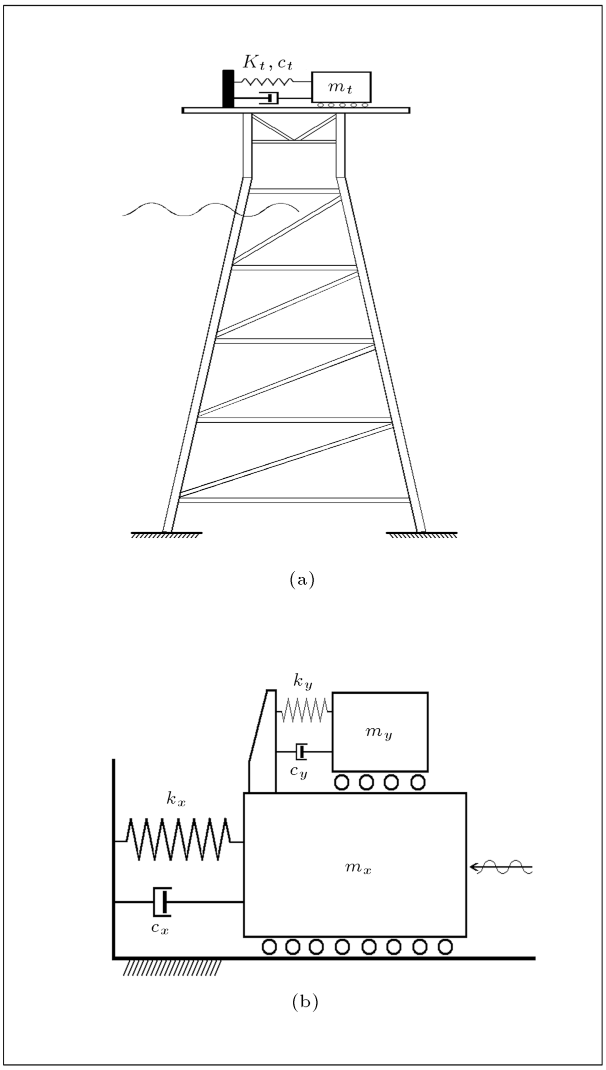

Figure 13. Steel jacket platform utilized with a TMD and its equivalent SDOF system.

$$\mu = \frac{m_y}{m_x}, \qquad \xi_x = \frac{c_x}{2m_x\omega_x}, \qquad \xi_y = \frac{c_y}{2m_y\omega_y},$$

$$\omega_x = \sqrt{\frac{k_x}{m_x}}, \qquad \omega_y = \sqrt{\frac{k_y}{m_y}},$$

where μ is the mass ratio between TMD and the SDOF system; ξ_x and ω_x are the damping ratio and the natural frequency for the SDOF, respectively; and ξ_y and ω_y are the same for the auxiliary control mechanism.

The efficiency of TMDs in the reduction of vibration amplitude was first investigated by Den Hartog [20]. Warburton [21] completed his studies to find the optimum parameters for TMDs attached to undamped SDOF systems subjected to various types of excitation, such as harmonic force, harmonic support motion or white noise random excitations. In all cases, the object is to bring the resonant peak of the amplitude down to its lowest possible value, which leads to optimum parameters. In the case of white noise excitation, setting the derivatives of the response function, with respect to ω_y and ξ_y, equal to zero, results in optimal tuning and damping parameters for the TMD device:

$$\omega_{y\text{ opt}} = \omega_x \frac{\sqrt{1+\mu/2}}{1+\mu},$$

$$\xi_{y\text{ opt}} = \sqrt{\frac{\mu(1+3\mu/4)}{4(1+\mu)(1+\mu/2)}}. \tag{34}$$

All the above mentioned optima have been derived under simplifying assumptions for a primary structure and imposed excitations, so they are only dependent on the mass ratio while practical applications confront other types of response and excitation which lead to more complicated optimization problems that can be solved by numerical schemes. An offshore platform which is under sea wave excitation is one of these cases.

The expected value of topside displacement can be found by using the transfer function of the wave load, $H_{f\zeta}(\omega)$, and the wave spectrum by:

$$E[x^2] = \int_{-\infty}^{+\infty} \left|H_{x\zeta}(\omega)\right|^2 S_\varsigma(\omega)d\omega. \tag{35}$$

The optimal tuning and damping parameters of the auxiliary device that minimize this equation are also dependent on the shape of the wave spectrum in addition to the dynamic characteristics of the primary structure, and this is the major concern of this study in comparison with traditional and seismic application of TMDs. From the two common parameters used to describe a wave spectrum, the mean zero up crossing period of waves T_z evidently affects the optimal values

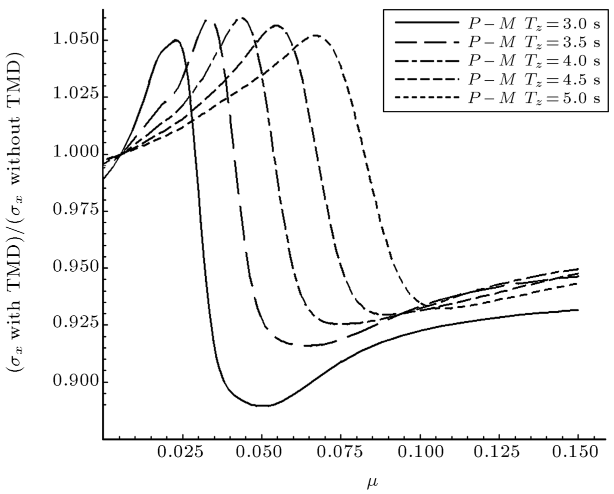

Figure 14. Suppression of the displacement range by a TMD with a constant stiffness $ky = 0.02\ kx$ and damping $\xi y = 0.02$.

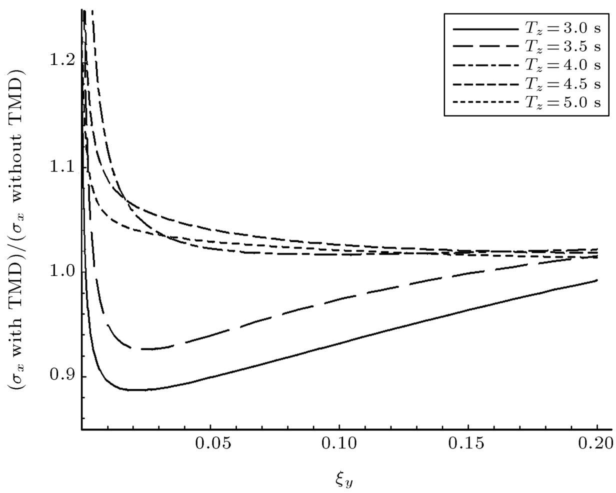

Figure 16. Suppression of the displacement range by a TMD with a constant mass ratio $\mu = 0.05$ and stiffness $ky = 0.02\ kx$.

of these parameters and this is apparent in Figure 14 which demonstrates the efficiency of a TMD for suppression of the vibration in a SDOF system excited with random waves described with a P-M spectrum. The natural frequency of the corresponding primary system is $\omega_x = 2.0$ rad/sec. Although using the TMD with $\mu > 0.1$ has a positive performance in all sea-states, in a practical range of mass ratios, the functionality of TMD is very sensitive to sea-state conditions.

The zero up-crossing periods of the exciting waves also affect the optimal tuning ratio of TMD as shown in Figure 15, but according to Figure 16, it does not have a considerable effect on the optimal value of the TMD damping ratio.

It is well known that passive control systems are only operative for structures with a remarkable dynamic response, whereas for low rise platforms, the quasi static response contribution becomes dominant, because their effective frequency band of dynamic response stands apart from the narrow frequency band of the wave induced forces PSD function as shown in Figure 17. Therefore, an optimally designed TMD to moderate the peak value of the response function of such a primary structure does not necessarily reduce the variance of the displacement response under sea wave excitation, and the optimal tuning of TMD is dependent on the peak frequency of the exciting spectrum as is clear in Figure 18a.

Further overlapping of the frequency response function and the exciting forces spectrum raises the efficiency of TMD as is clear in Figure 18b. However, the dependency of optimal tuning on the peak frequency of

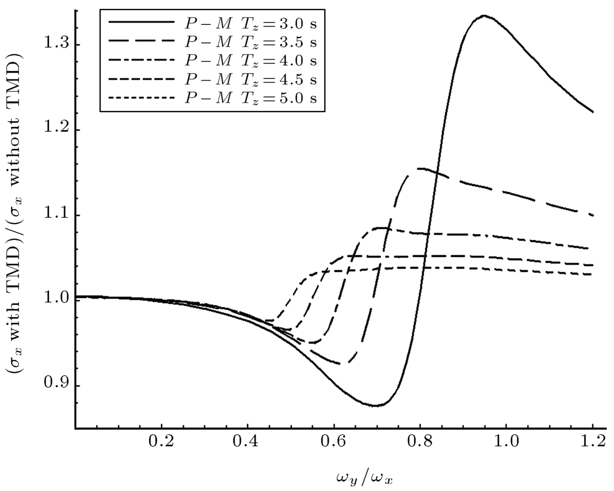

Figure 15. Suppression of the displacement range by a TMD with a constant mass ratio $\mu = 0.05$ and damping $\xi y = 0.02$.

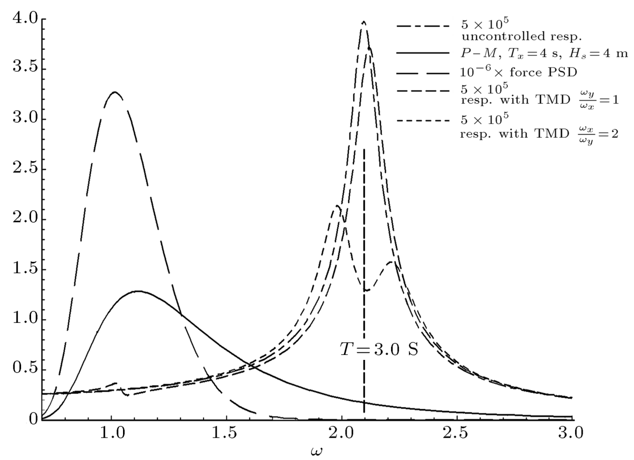

Figure 17. Wave height and resultant forces PSD functions and controlled and uncontrolled SDOF systems' frequency response functions.

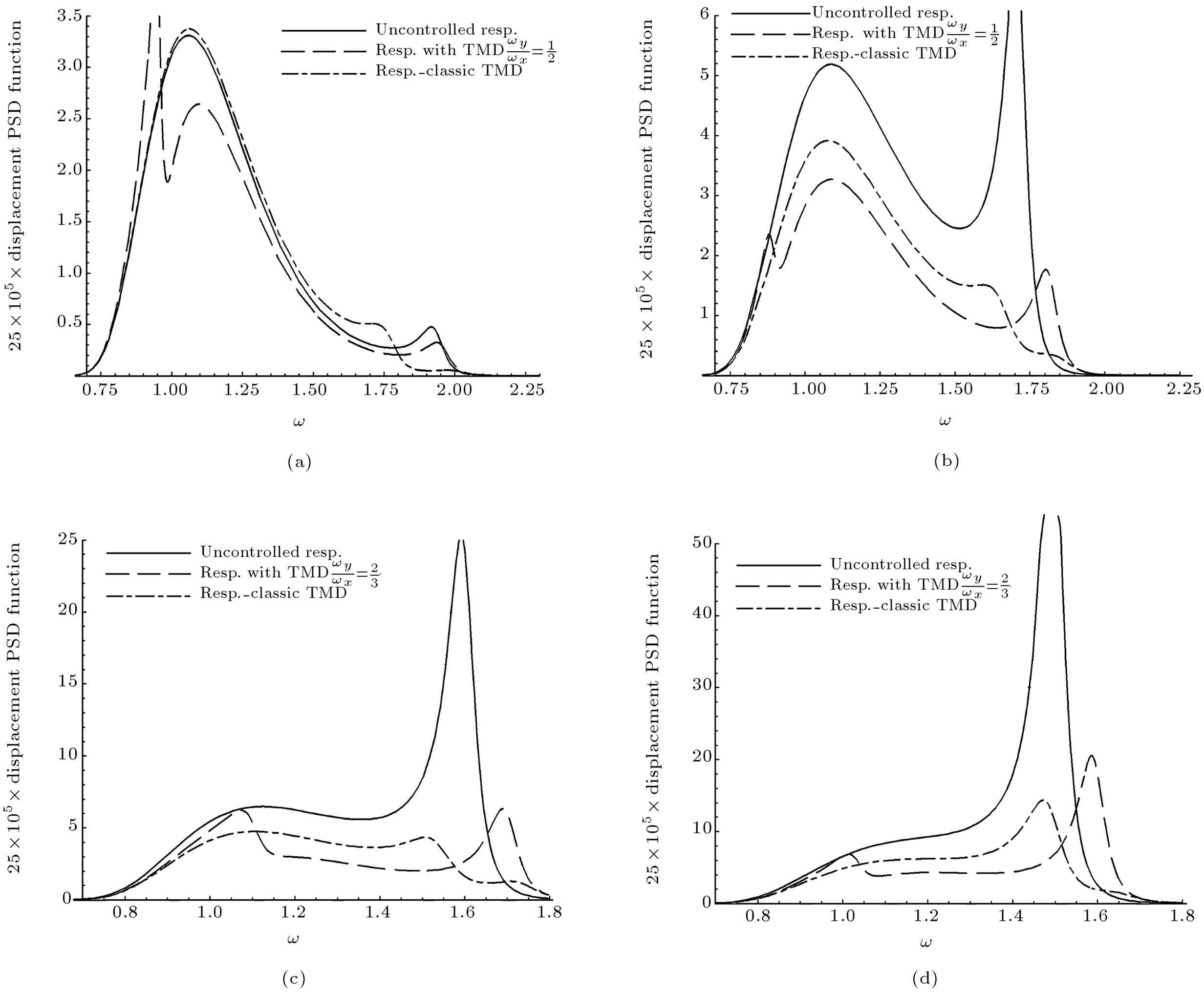

Figure 18. Displacement response PSD functions for a SDOF system considering $P-M$ spectrum with $Tz = 4.0$ s and $Hs = 4.0$ m for exciting waves. (a) $T = 3.25$ s; (b) $T = 3.5$ s; (c) $T = 3.75$ s and (d) $T = 4.0$ s.

the exciting forces spectrum persists up to the nearness of the natural frequency of the structure to the peak frequency of the exciting forces spectrum, and this is discernible from Figure 18c. But, in close vicinity to these two frequencies, suppression of the peak value of the response function finds more relevancy.

The optimal parameters for a TMD to minimize the displacement response of a SDOF under random excitations can be determined by numerical approaches.

According to the foregoing discussions, the optimum TMD parameters to moderate the displacement response of fixed offshore platforms under sea wave excitations are dependent on the sea-state, whereas the high probability of occurrence for moderate sea-states raises their participation in fatigue damage accumulation. Furthermore, a large amount of kinetic energy is exerted on the structure in savage sea-states, so all sea-states are decisive in fatigue damage accumulation in offshore structures and the deficiency of the control system in each sea-state may taint its performance in fatigue damage mitigation. Improvement in the functionality of the TMD for fatigue damage mitigation in an offshore platform has been summarized in Table 2. The generalized mass, associated with the principal dynamic mode of the platform and the corresponding frequency of vibration, has been considered as the parameters of the primary SDOF system. The P-M wave height spectrum with parameters related to open seas and a North Atlantic wave scatter diagram has been employed in these calculations.

The efficiency of the control system is defined as:

$$\text{Efficiency} = 1 - \frac{\text{fatigue damage with control mechanism}}{\text{fatigue damage without control mechanism}}.$$

In the studied model, using the optimum mass for the TMD device in each sea-state has caused a significant improvement in its performance.

Table 2. Variable mass TMD and its functionality in comparison with constant TMD for a primary structure with $m_x = 2450$ tons, $\omega_x = 2.1$ rad/sec and $\xi_x = 3\%$.

Sea-State Definition		**Sea-State Occurrence**	**Efficiency of Constant TMD, $\mu = 0.05$**	**Optimal TMD $k_y = 0.024k_x$,**	**Optimal TMD**
T_z sec	**H_s m**	**(%)**	**$k_y = 0.024k_x$, $c_y = 0.05c_x$**	**$c_y = 0.05c_x$**	**Efficiency**
1.95	0.30	7.2	39.0%	$\mu = 0.024$	45.2%
3.34	0.88	22.4	35.1%	$\mu = 0.025$	43.1%
4.88	1.88	28.7	32.0%	$\mu = 0.034$	36.5%
6.42	3.25	15.5	28.1%	$\mu = 0.055$	33.2%
7.96	5.00	18.7	12.3%	$\mu = 0.064$	31.7%
9.75	7.50	6.1	2.5%	$\mu = 0.075$	30.2%
12.07	11.50	1.2	-4.5%	$\mu = 0.081$	29.3%
13.32	14.00	0.2	-11.4%	$\mu = 0.085$	28.5%
Aggregative:			26.6%		36.7%

CONCLUSION

Analytical studies have been performed aiming to evaluate and compare the efficiency of friction dampers and TMDs as passive devices for fatigue damage mitigation in offshore steel jacket platforms.

Although the efficiency of both dissipative systems increases for more flexible platforms due to the dominancy of the dynamic response, the functionality of TMD devices is more dependent on the dynamic characteristics of the platform; and friction dampers seem to be more efficient for fixed steel jacket platforms.

Optimal values for the adjustable parameters of the TMD are strongly dependent on sea-state conditions defined with wave spectrum parameters, T_z and H_s. Using the optimal tuning ratio for each sea-state causes a considerable increase in TMD efficiency and, considering the predictability of sea-states, this can be addressed as an advantage for offshore application of TMDs, in comparison with their seismic applications.

An optimally regulated friction damper results in a considerable reduction in the topside displacement variance and the variance of its velocity. This predicates an excellent effectuality of friction dampers for prolonging the fatigue life of this type of offshore platform.

As a case study, the efficiency of TMD has been examined to moderate the dynamic response of a realistic jacket type platform. The utilization of optimally tuned TMD on this platform resulted in a 26.6% reduction in maximum fatigue damage. This efficiency can be increased up to 36.7%, using variable tuning of the auxiliary device in each sea-state.

REFERENCES

1. Spencer, B.F. Jr. and Nagarajaiah, S. "State of the art of structural control", *ASCE Journal of Structural Engineering*, **129**(7), pp. 845-856 (July 2003).
2. Abdel-Rohman, M. "Structural control of a steel jacket platform", *Structural Engineering and Mechanics*, **4**(2), pp. 125-138 (1996).
3. Terro, M.J., Mahmoud, M.S. and Abdel-Rohman, M. "Multi-loop feedback control of offshore steel jacket platforms", *Computers and Structures*, **70**(2), pp. 185-202 (1999).
4. Suhardjo, J. and Kareem, A. "Feedback-feedforward control of offshore platforms under random waves", *Earthquake Engineering and Structural Dynamics*, **30**, pp. 213-235 (2001).
5. Li, H.-J., Hu, S.L.J. and Jakubiak, C. "H_2 active vibration control for offshore platform subjected to wave loading", *Journal of Sound and Vibration*, **263**(4), pp. 709-724 (2003).
6. Zribi, M., Almutairi, N., Abdel-Rohman, M. and Terro, M. "Nonlinear and robust control schemes for offshore steel jacket platforms", *Nonlinear Dynamics*, **35**(1), pp. 61-80 (January 2004).
7. Ma, H., Tang, G.Y. and Zhao, Y.D. "Feedforward and feedback optimal control for offshore structures subjected to irregular wave forces", *Ocean Engineering*, **33**, pp. 1105-1117 (2006).
8. Hsien Hua Lee "Stochastic analysis for offshore structures with added mechanical dampers", *Ocean Engineering*, **24**(5), pp. 817-834 (1997).
9. Patil, K.C. and Jangid, R.S. "Passive control of offshore jacket platforms", *Ocean Engineering*, **32**, pp. 1933-1949 (2005).
10. Kazakov, I.E. "Generalization of the method of statistical linearization to multidimensional systems", *Automatic Remote Control*, **26**, pp. 1201-1206 (1965).
11. Caughey, T.K. "Random excitation of a system with bilinear hysteresis", *ASME Journal of Applied Mechanics*, **27**, pp. 649-652 (1960).

12. Socha, L. "Linearization in analysis of nonlinear stochastic systems: Recent results - Part I: Theory", *ASME Journal of Applied Mechanics*, **58**, pp. 178-205 (2005).

13. Socha, L. "Linearization in analysis of nonlinear stochastic systems: Recent results - Part II: Applications", *ASME Journal of Applied Mechanics*, **58**, pp. 303-315 (2005).

14. Atalik, T.S. and Utku, S. "Stochastic linearization of multi degree of freedom nonlinear systems", *Earthquake Engineering and Structural Dynamics*, **4**, pp. 411-420 (1976).

15. Mualla, I.H. and Belev, B. "Performance of steel frames with a new friction damper device under earthquake excitation", *Engineering Structure*, **24**, pp. 365-371 (2002).

16. Chakrabarti, S.K., *Hydrodynamics of Offshore Structures*, Computational Mechanics Publications (1994).

17. Yang, C.Y., *Random Vibration of Structures*, John Wiley & Sons, USA (1985).

18. Dalane, J.I. "System reliability in design and maintenance of fixed offshore structures", Ph.D. Thesis, Norges Tekniske Hogskole, Trondheim, Norway (1993).

19. Holmes, D. "Listing of installations", *Engineering Structures*, **17**, pp. 676-677 (1995).

20. Den Hartog, J.P., *Mechanical Vibrations*, New York, McGraw-Hill (1956).

21. Warburton, G.B. "Optimum absorber parameters for various combinations of response and excitation parameters", *Earthquake Engineering and Structural*, **10**, pp. 381-401 (1982).